Infrared spectroscopy of large ammonia clusters as a function of size

Christof Steinbach and Udo Buck[a)]
Max-Planck-Institut für Dynamik und Selbstorganisation, Bunsenstrasse 10, 37073 Göttingen, Germany

Titus A. Beu
Department of Theoretical Physics, University "Babeş-Bolyai," 3400 Cluj-Napoca, Romania

(Received 3 April 2006; accepted 1 August 2006; published online 3 October 2006)

We have measured the vibrational spectra of large ammonia $(NH_3)_n$ clusters by photofragment spectroscopy in the spectral range from 3150 to 3450 cm^{-1} for the average sizes $\langle n\rangle=29$, 80, 212, 447, and 989 and by depletion spectroscopy for $\langle n\rangle=8$. The spectra are dominated by peaks around 3385 cm^{-1} which are attributed to the asymmetric ν_3 NH-stretch mode. Two further peaks between 3200 and 3260 cm^{-1} have about equal intensity for $\langle n\rangle=8$ and 29, but only about 0.40 of the intensity of the ν_3 peak for the larger sizes. The spectra for the smallest and largest size agree with those obtained by Fourier transform infrared spectroscopy in slit jet expansion and collision cells, respectively. By accompanying calculation we demonstrate that the energetic order of the spectral features originating from the bending overtone $2\nu_4$ and the symmetric NH-stretch ν_1 in the range from 3150 to 3450 cm^{-1} is changed between $n=10$ and 100, while the asymmetric NH-stretch ν_3 only exhibits a moderate redshift. The reason is the coupling of the ground state modes to the overtones. © *2006 American Institute of Physics*. [DOI: 10.1063/1.2345057]

I. INTRODUCTION

Ammonia is an important solvent molecule which is able to form hydrogen bonded networks. In addition, it is a prominent component of the atmospheres of several planets in the solar system.[1] It condenses into a cubic lattice with six nearest neighbors, all of which are hydrogen bonded.[2] Each of the three hydrogen atom donors forms a single bond and the lone pair of the nitrogen accepts another three bonds. A sensitive probe of this hydrogen bonded network is usually the spectroscopy of the vibrational NH-stretch mode which undergoes a redshift upon the hydrogen bonding. A closer inspection of the corresponding energy range between 3200 and 3500 cm^{-1} reveals that, aside from the expected asymmetric stretch $\nu_3(E')$ and symmetric stretch $\nu_1(A_1')$, also the overtone of the asymmetric bending mode $2\nu_4(A_1'+E')$ is experimentally observed in this spectral region. It is coupled by a Fermi resonance to the ν_1 mode. Therefore it is very instructive to compare the frequencies of the spectral origins of the gas phase molecule NH_3 for the infrared absorption, $\nu_3=3444$ cm^{-1}, $\nu_1=3336$ cm^{-1}, and $2\nu_4=3217$ and 3240 cm^{-1},[3,4] with those of the crystalline solid, $\nu_3=3375$ cm^{-1}, $2\nu_4=3290$ cm^{-1}, and $\nu_1=3210$ cm^{-1}.[5–7] Aside from the already mentioned redshift for ν_3, we notice that the ordering in the energy between ν_1 and $2\nu_4$ has been reversed. This assignment has been discussed at length in the literature,[6] but based on the intensity distributions and the corresponding Raman spectra there is now general agreement about it.[8] Similar conclusions have been drawn for the liquid. Here the Fermi resonance between the ν_1 and the $2\nu_4$ mode was analyzed and, from the temperature dependence of the lines, the same ordering was determined.[9] We also note that in the IR spectra of the condensed phase the intensity of the ν_3 mode is much larger than that of the two other modes, in contrast to the gas phase spectrum of the molecule where all three modes show roughly equal intensity.

Although the reverse ordering of the two modes between the gas and the condensed phase is now well established, a consistent explanation of the effect was to our knowledge not yet presented. Here the behavior of ammonia clusters comes into play. There is currently great interest in ammonia clusters. Infrared spectra of small complexes were measured for the umbrella[10] and the NH-stretch[11] mode. Large aerosol particles[12] and clusters solvated in helium droplets[13] have been measured in the region of the NH-stretch vibration. In addition, Raman spectra are available.[14] They should definitely exhibit this effect in detail when the size is gradually increased. But most of these data do not vary the sizes over an appreciable range. An exception are the measurements in helium droplets which cover sizes up to $\langle n\rangle=900$, but with a preference for the smaller ones.[13] Theoretically, we recently calculated the IR spectra of small ammonia clusters up to $n=20$ and found that the two stretching modes display a redshift, while the umbrella bending mode ν_2 is blueshifted, since its motion perpendicular to the bond direction weakens the hydrogen bond.[15,16] Thus a simple picture might explain the reverse ordering of the two modes. The ν_1 and the ν_3 as stretching modes shift to smaller energies, to the red, while $2\nu_4$ as bending mode shifts to larger energies, to the blue, upon increasing the cluster size and thus the hydrogen bonding network. At a particular range of cluster sizes the two spectral patterns should cross.

To investigate this model, we have measured the IR spectra of ammonia clusters in the range from 3150 to 3450 cm^{-1} for the average sizes from $\langle n\rangle=8$ to 989. In this way we cover, for the first time, the whole range from

a)Author to whom correspondence should be addressed. Electronic mail: ubuck@gwdg.de

small aggregates to aerosol particles. Aside from the spectrum for $\langle n\rangle=8$ which is obtained by depletion spectroscopy, we apply the method of photofragment spectroscopy which was pioneered by Vernon *et al.*[17] and recently also successfully applied to large water clusters.[18] The size distributions are known from another technique introduced by us, the doping with sodium atoms.[19] To analyze these measurements we also had to extend our calculations to larger cluster sizes and to include the overtone of the asymmetric bending mode $2\nu_4$. As will be shown in detail, the calculations and the measurements confirm the predicted crossover of the redshifted ν_1 and the nearly constant $2\nu_4$ mode. In the calculations, which were based on the model described in Ref. 15, the coupling to closely lying overtones had to be taken into account to observe this behavior.

II. EXPERIMENTAL METHODS

The experiments have been carried out in a molecular beam machine which has been described in detail previously.[20,21] The large ammonia clusters are produced in a supersonic expansion of pure ammonia vapor at 0.45–6 bars through nozzles of conical shape with diameters of 60 and 90 μm, opening angles of 20.4° and 41°, and lengths of 2 and 6 mm. The average size of the cluster distribution is determined by applying the recently developed method of doping the cluster by the pickup of Na atoms.[19] In this way the cluster can be ionized free of fragmentation by single photons close to the threshold. The clusters follow a log-normal distribution with a width which approximately corresponds to the average size. Based on a series of such results we have derived a scaling law[19] which relates the mean cluster size $\langle n\rangle$ to the source conditions of the expansion in the spirit of the well known scaling laws derived by Hagena for rare gases and metals.[22,23] The key parameter that correlates the flow which produces the same cluster size is given by

$$\Gamma = n_0 d^q T_0^\alpha \quad (0 < q \leqslant 1). \tag{1}$$

Here n_0, T_0, and d are the source density, nozzle temperature, and nozzle diameter. For ammonia clusters we get $q=0.704$ and $\alpha=-3.300$. For nozzles with conical shape and an opening angle of 2β, the nozzle diameter d has to be replaced by $d_{\mathrm{eff}}=0.933/\tan\beta$. It is convenient to reduce the length and energy scale by introducing the reduced parameter $\Gamma^*=\Gamma/(r_{\mathrm{ch}}^{q-3}T_{\mathrm{ch}}^\alpha)$, with $r_{\mathrm{ch}}=3.20$ Å and $T_{\mathrm{ch}}=3510$ K. Then we are able to present the relation of the average cluster size $\langle n\rangle$ with the reduced source parameter Γ^* by a simple power law:

$$\langle n\rangle = D\left(\frac{\Gamma^*}{1000}\right)^a, \tag{2}$$

with $D=1.09$ and $a=1.246$. In this way the sizes of ammonia clusters generated in adiabatic nozzle expansions can be calculated from the source parameters. The results are listed in Table I.

The vibrational spectra of the large ammonia clusters $(NH_3)_n$ are measured in the following schematic experimental arrangement. The pulsed infrared optical parametric oscillator (OPO) output crosses the cluster beam in a quasicollinear configuration under a small angle of 3° and is tuned in a frequency range of 3100–3460 cm^{-1} with a bandwidth of 0.2 cm^{-1}. The laser fluence was kept constant at 250 $\mathrm{mJ/cm}^2$ in a single pulse. If a vibrational mode of the clusters is excited, the energy is redistributed and leads to the decay of the cluster. For these large clusters the detection of the fragment is much more appropriate than the depletion method usually used for small clusters.[24] Therefore the detector, a rotatable quadrupole mass filter with a continuous electron bombardment ion source, is positioned at an angle Θ of 3° with respect to the ammonia cluster beam. A chopper allows digital lock-in measurements to discriminate the signal of the continuous ammonia cluster beam from background. Neutral fragments are leaving the clusters and thereby diverging from the direction of the ammonia cluster beam. Then they are detected as enhancement of the signal following the laser pulse in the time resolved ion signal of the tuned masses. For the smallest cluster size $\langle n\rangle=8$ a slightly different procedure is used. Here the conventional depletion spectroscopy is applied[24] with the detector placed at 0° and the mass filter tuned to the mass $(NH_3)_5H^+$. In this way, all neutral cluster contributions $n<6$ are precluded. Because of possible fragmentation processes,[25] the average value is estimated to $\langle n\rangle=8$. This procedure implies a partial size selection which does not explicitly depend on the source condition. We have used the conditions of experiment 1 of Table I for this experiment.

TABLE I. Beam data.

Property	Expt. 1	Expt. 2	Expt. 3	Expt. 4	Expt. 5
Nozzle diameter d (μm)	90	90	90	90	60
Opening angle 2β (deg)	41	41	41	41	20.4
Nozzle length (mm)	2	2	2	2	6
Nozzle temperature (K)	307	307	307	307	307
Pressure (bar)	0.45	1.0	2.2	4.0	6.0
Average size $\langle n\rangle$	29	80	212	447	989

III. EXPERIMENTAL RESULTS

The vibrational modes of the ammonia clusters are excited by the pulsed IR radiation and the resulting predissociation is detected by counting the emitted fragments. The result obtained for the average cluster size $\langle n\rangle=80$ and the excitation at 3380 cm^{-1} is shown in Fig. 1. Because of the electron impact ionization, protonated ions appear. The fragment with the smallest mass has the largest intensity and the distribution decreases monotonically with increasing mass. Such a result is expected from statistical considerations, as was demonstrated in extensive calculations for water clusters.[18] Interestingly, this result is different from the experimental findings for water clusters in this size range where the maximum was observed for water hexamers.[18] For measuring the infrared spectra, the quadrupole mass filter was tuned to the mass of $(NH_3)_5H^+$. This is a compromise between the larger intensity at the smaller masses and the lower background from hydrocarbons at larger masses. We note that, because of fragmentation problems by the electron impact ionization, the most probable neutral precursor is $(NH_3)_7$.[25]

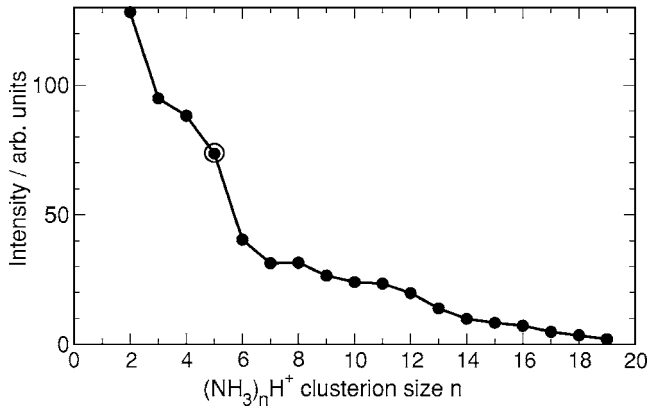

FIG. 1. Measured intensity dependence of the cluster ion fragment size. The encircled mass was used in the experiment.

As further check of the process we have measured the dependence of the fragment ion signal $(NH_3)_5H^+$ on the cluster size at the excitation of the NH-stretching mode at 3380 cm^{-1}. The result is presented in Fig. 2. We observe a pronounced size dependence. The distribution rises from $\langle n\rangle=20$ to about $\langle n\rangle=80$, and then falls off to $\langle n\rangle=200$ where a change in the slope occurs. A possible explanation for the size dependence is simply the size of the fragment. For such a large fragment, low-coordinated molecules are energetically favored, since a smaller number of bonds have to be broken. Therefore the increase of the IR intensity with cluster size can be explained by the increasing number of undercoordinated molecules. Based on the results of Ref. 16 Sec. IV we estimate the number of undercoordinated (from two- to five-coordinated) molecules to 15 for $n=16$ and 69 for $n=100$. This trend, however, continues, although somewhat weakened for $n=500$ and $n=1000$ where 225 and 357 undercoordinated molecules are counted, respectively. Apparently, the intensity goes down after $n=100$. This decrease is explained by the increasing number of six-coordinated molecules which appear at the expense of the undercoordinated ones at the surface. In the investigated size range the percentage of undercoordinated molecule decreases from 94% for $n=16$ over 69% for $n=100$ to 45% for $n=500$ and 36% for $n=1000$. Thus these two conflicting trends are responsible for the maximum in the intensity as function of the cluster size. We note that the preference for undercoordinated molecules in the detection process leads to a preferred sensitivity to the surface, since most of these molecules are found in the surface region. Their fraction is 100% for the small clusters and about 85% around the cluster size of $n=1000$.

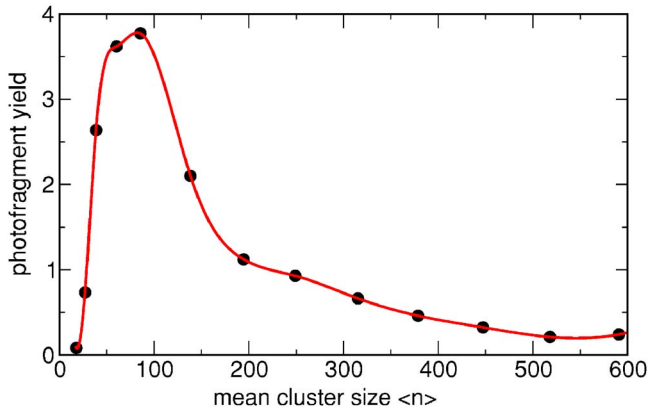

FIG. 2. (Color online) Measured cluster size dependence of the photofragment intensity at the infrared frequency of 3385 cm^{-1}.

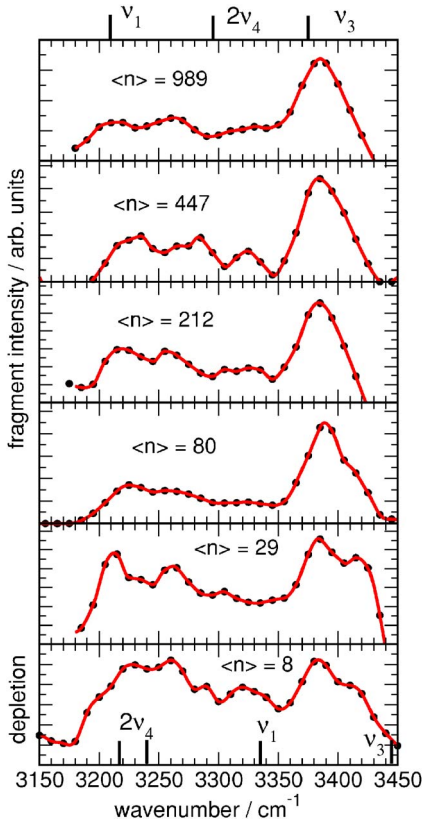

FIG. 3. (Color online) Measured IR fragment spectra detected at $(NH_3)_5H^+$ for the average sizes indicated. The spectrum at the bottom is taken by depletion. The positions of the three vibrational modes in this frequency range are marked by bars, at the bottom, for the gas phase spectrum of a single molecule, and, at the top, for the condensed phase. These are the asymmetric NH-stretch mode ν_3, the symmetric NH-stretch mode ν_1, and the overtone of the asymmetric bending mode $2\nu_4$.

We have measured the vibrational predissociation spectra after the excitation in the infrared spectral range from 3150 to 3450 cm^{-1}. The average cluster sizes include $\langle n\rangle=8$, 29, 80, 212, 447, and 989. The results are presented in Fig. 3. The spectra for all sizes, aside from the two smallest ones, are dominated by the peak at 3385 cm^{-1}. For the average sizes $\langle n\rangle=29$ and $\langle n\rangle=8$ we observe about equal intensity of this peak and peaks between 3200 and 3270 cm^{-1}. Signals in this wave number range are also present at the other sizes from $\langle n\rangle=80$ to $\langle n\rangle=989$ but with about 40% of the intensity of the peak at 3385 cm^{-1}. This peak, which is attributed to the asymmetric NH-stretching mode, does not change the position over the measured size range. A shoulder at 3400 cm^{-1} which is present at the smaller cluster sizes disappears for the larger clusters. The two peak structure in the range from 3210 to 3270 cm^{-1} is more or less present over the whole size range measured.

We can compare the present data taken at the smallest and largest cluster sizes with those obtained by Fourier transform infrared (FTIR) spectroscopy in slit jet expansions of

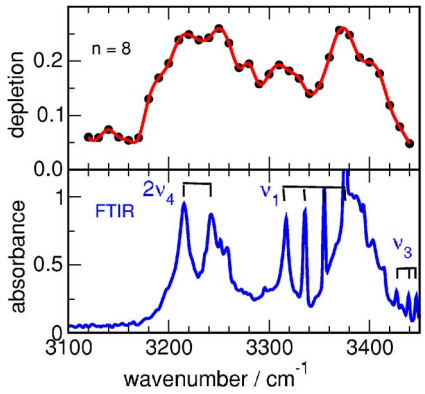

FIG. 4. (Color online) Comparison of the present data for $\langle n\rangle=8$ (upper panel) with those obtained in slit expansion by the FTIR jet method of Ref. 11 (lower panel). The narrow peaks marked by bars are rotational lines of the monomer NH_3 belonging to the indicated vibrational modes.

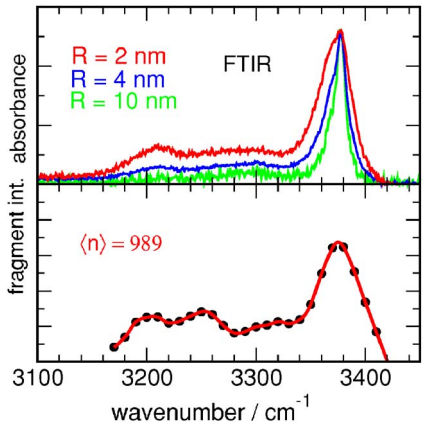

FIG. 5. (Color online) Comparison of the present data for $\langle n\rangle=989$ (lower panel) with those obtained in collision cells of Ref. 12 (upper panel). The estimated sizes of the FTIR experiment refer to the curves from top to bottom. The spectrum of the aerosol particle of the radius 2 nm corresponds to the average size $\langle n\rangle=1027$.

Liu *et al.*[11] and in collision cells by Jetzki *et al.*[12] This is quite interesting, since the FTIR data exhibit the correct absorption properties, while the present data obtained by depletion or fragment spectroscopy measure a convolution of the absorption and the subsequent dissociation process. The comparison for $\langle n\rangle=8$ is shown in Fig. 4. Given the different expansion conditions and the different methods of data sampling, the agreement is remarkable. The spikes in the FTIR data are monomer lines which can be easily assigned to the marked position of the three vibrational modes. The two lines in the range of the $2\nu_4$ mode and the lowest wave number ν_1 mode coincide with the cluster modes and lead to a better resolution in the FTIR experiment,[11] but the general features of the three groups of lines are identical. From the depletion data we explicitly know that no clusters $n<6$ are present in the beam. This provides us also with a lower limit for the cluster size of the FTIR jet experiment. The outermost monomer lines above 3400 cm^{-1} belong to the ν_3 mode. The redshift of the cluster modes is clearly observed. The next four monomer lines between 3310 and 3380 cm^{-1} are indications of the ν_1 mode. The lines below 3260 cm^{-1} are caused by the overtone of the $2\nu_4$ mode. Since we do not know at this moment which of the cluster peaks belongs to which mode, we have to postpone the discussion of the direction of the shifts after the presentation of the results of the theory.

The comparison at the upper end of the size scale is shown in Fig. 5. The result of the fragment spectroscopy of the present work for $\langle n\rangle=989$ agrees well with the measured curve of the aerosol particles of the radius $R=2$ nm which corresponds to an average size of $\langle n\rangle=1027$.[12] The positions and the widths of the peaks at 3380 and 3210 cm^{-1} are nearly identical. They are attributed in this size range by comparison with the condensed phase data to the asymmetric ν_3 and the symmetric ν_1 mode, respectively. The intensity in between is attributed to the $2\nu_4$ mode. Even the trend in the intensity ratio of the peaks at 3210 and 3380 cm^{-1} is reproduced with 0.25 for the FTIR and 0.38 for the fragment experiment.

This is a notable result. There is a big difference compared to the results of water clusters for which the spectra measured by fragment spectroscopy differ appreciably from those obtained in collision cells by FTIR spectroscopy.[18,26] The reason for this behavior is the pronounced sensitivity of the cluster fragment spectroscopy to the outer surface. It originates from the fact that the measured fragment mass $(H_2O)_4H^+$ had the largest intensity and that the surface region was amorphous compared to the interior of the cluster. Both properties favor the formation of large connected low-coordinated molecules at the surface. For ammonia clusters both conditions are not fulfilled. The structure for the larger clusters is also crystalline at the surface[27] and the smallest fragment size has the largest intensity (see Fig. 1). Nevertheless for ammonia clusters in the present experiment, there is a certain sensitivity to the surface left which is caused by the large fragment mass and the subsequent preference of undercoordinated molecules as was discussed earlier. But it is much less pronounced than in the case of water clusters.

A different way to look at this problem is to calculate the ratio of the intensity of the ν_1 and the $2\nu_4$ mode to the ν_3 mode. The results give for the measurements of Fig. 3 2.02 for $\langle n\rangle=8$, 1.36 for $\langle n\rangle=29$, 0.83 for $\langle n\rangle=80$, 1.00 for $\langle n\rangle=212$, 0.92 for $\langle n\rangle=447$, and 0.86 for $\langle n\rangle=989$. As expected, the intensity of the ν_3 mode becomes more and more significant. The value for the smallest cluster is in good agreement with the very precise most recent measurement of this ratio of 2.2 of the transition moments of the monomers.[28] The one for the largest cluster agrees well with the ratio 0.94 which is obtained for the FTIR spectra of the aerosol particles of the average size $\langle n\rangle=1027$.[12] The ratios for the larger clusters from $\langle n\rangle=80$ onwards are within the experimental errors the same. This is a clear indication that they are dominated by surface effects. In contrast, in the aerosol experiments of Jetzki *et al.*[12] this ratio drops from 0.94 for the 2 nm to 0.72 for the 4 nm and to 0.48 for the 10 nm particles. This trend continues finally to the results of the crystalline solid where still lower values around 0.35 are observed.[5,7] The reason is a cancellation of the effective oscillatory dipole of the ν_1 mode in the highly symmetric arrangement of the molecules in the unit cell of the crystal.[5] Consequently this trend is not

observed for the amorphous solid phase[7] where the intensity of the ν_1 and the $2\nu_4$ mode slightly exceeds that of the ν_3 mode. A similar trend is observed by the width of the peak of the ν_3 mode at 3385 cm^{-1}. It is quite broad for the clusters up to $n=1000$ and becomes very sharp for the crystal. In this sense our data confirm the conclusions of Jetzki *et al.*[12] that the decreasing width of the peak at 3380 cm^{-1} and decreasing intensity of the peak at 3210 cm^{-1} for larger cluster sizes are caused by reduced influence of surface effects.

The good agreement of the present data with FTIR experiments in the limit of small and large cluster sizes gives us confidence that the data in between are also reliable and can be used to explain the change in the infrared signature of ammonia clusters.

IV. THEORETICAL METHODS AND RESULTS

The calculations included (1) computations of the minimal energy structures of the clusters using stochastic methods and simulated annealing embedded in classical molecular dynamics simulations, and (2) quantum calculations of the line shift of the vibrational spectra employing a model based on perturbation theory.[29,30] The NH_3–NH_3 intermolecular potential used in our calculations is the site-site model of Impey and Klein.[31] The NH_3 monomer is considered rigid. Each molecule features four electrostatic interaction sites and additional Lennard-Jones interactions between the N atoms. It was extensively used in molecular dynamics simulation of the liquid and reproduces the x-ray and neutron diffractions satisfactorily.[32]

Our formalism for the frequency shifts of molecular clusters[29,30,33] is based on the idea of treating the anharmonic intramolecular force field and the intermolecular potential as perturbation of the molecular vibration, described in the normal mode approach. It was successfully applied to several systems, including ammonia clusters up to $n=20$.[15,16] For a homogeneous cluster formed of n molecules, the first order frequency shifts $\Delta\nu_{mi}^{(1)}$ relative to a particular vibrational mode m of the monomer i were shown to result by solving an eigenvalue problem:

$$\sum_{m'\in\Gamma}\sum_{i'=1}^{n}\left(\frac{\partial^2 U}{2\partial q_{mi}\partial q_{m'i'}}-hc\Delta\nu_{mi}^{(1)}\delta_{mm'}\delta_{ii'}\right)c_{m'i',mi}=0,$$
$$i=1,2,\ldots,n. \tag{3}$$

The perturbation matrix elements are expressed in terms of the curvature $\partial^2 U/\partial q_{mi}\partial q_{m'i'}$ of the intermolecular potential U. q_{mi} is the normal coordinate associated with normal mode m of molecule i. In the case of a degenerate mode both m and m' belong to the subspace Γ of the considered normal mode, while for a nondegenerate mode $m\equiv m'$.

The second order line shifts can be explicitly expressed as

$$\Delta\nu_{mi}^{(2)}=\sum_{m',m''\in\Gamma}\sum_{i',i''}c_{m'i',mi}c_{m''i'',mi}^{*}\Delta\nu_{m'i',m''i''}^{(2)}, \tag{4}$$

where the coefficients $c_{m'i',mi}c_{m''i'',mi}^{*}$ are components of the eigenvectors yielded by the eigenvalue problem (3), and the partial contributions $\Delta\nu_{m'i',m''i''}^{(2)}$ are given by

$$\begin{aligned}\Delta\nu_{m'i',m''i''}^{(2)}&=-\frac{\delta_{i'i''}}{2hc}\sum_{r}\frac{1}{\omega_r}\frac{\partial U}{\partial q_{ri'}}\phi_{m'm''r}\\&+\frac{1}{4(hc)^2}\sum_{r\notin\Gamma}\sum_{j}\frac{1}{\omega_m-\omega_r}\\&\times\frac{\partial^2 U}{\partial q_{m'i'}\partial q_{rj}}\frac{\partial^2 U}{\partial q_{m''i''}\partial q_{rj}}\\&-\frac{1}{4(hc)^2}\sum_{r}\sum_{j}\frac{1}{\omega_m+\omega_r}\frac{\partial^2 U}{\partial q_{m'i'}\partial q_{rj}}\frac{\partial^2 U}{\partial q_{m''i''}\partial q_{rj}}.\end{aligned} \tag{5}$$

Here ω_m and $\phi_{m'm''r}$ are harmonic frequencies and cubic force constants, respectively. The most significant second order contributions are generally due to the first term, coupling the generalized intermolecular forces $-\partial U/\partial q_{ri'}$ with the cubic intramolecular force constants $\phi_{m'm''r}$.

As a first step in incorporating the intramolecular force field in our perturbative frequency shift approach, the normal mode analysis of the ammonia monomer is carried out by the GF (kinetic and force constant) matrix method of Wilson *et al.*[34] In a second step, the transformation of the intramolecular force field from valence to normal coordinates is done by the L-tensor formalism of Hoy *et al.*,[35] yielding anharmonic monomer frequencies and transformed cubic force constants $\phi_{m'm''r}$. In particular, the intramolecular interactions within the NH_3 monomer are modeled by the anharmonic valence force field of Morino *et al.*[36] This intramolecular force field is not able to reproduce the experimental transition dipole moments of the ν_1 mode ($d=0.0263$ D) and the ν_3 mode ($d=0.0184$ D).[28] They are with $d=0.0446$ D and $d=0.193$ D, respectively, too large.

The equilibrium structures of the small ammonia clusters ($n=2$, 4, 10, and 20) have been determined by stochastic minimization of the total interaction energy, considering the clusters as being composed of rigid monomers. Actually, the local energy minima have resulted from optimizing the positions of the mass centers and the orientations (specified by Euler angles) of the molecules, starting from random initial configurations. Several tens (up to hundreds) of thousands of minimizations are necessary to obtain the global minimum for a particular cluster size and, with a view to calculate the averaged IR spectra, we have stored the lowest couple of hundreds of configurations.

The equilibrium configurations of the larger clusters considered in this study ($n=100$, 500, and 1000) have been determined by simulated annealing embedded in molecular dynamics. The initial configuration of each cluster species was chosen to be a sphere cut from crystalline ammonia (see Ref. 37). After an initial uniform heating at temperatures up to 200 K (by assigning random, properly normalized velocities to all molecules), the crystal spheres were relaxed for about 20 ps, by removing 0.01% of the total kinetic energy at each time step. By following this procedure, we have prepared 100 configurations for $(NH_3)_{100}$, 5 for $(NH_3)_{500}$, and 1 for $(NH_3)_{1000}$. The limiting (lowest and highest) binding ener-

TABLE II. Binding energies (in kJ/mol) of the $(NH_3)_n$ clusters for the most stable isomers, E_n^1, and for the highest energy isomer considered in the averaging process of the IR spectra, E_n^{high}. N_{config} is the number of configurations retained in the averaging of the IR spectra, corresponding to a temperature of 200 K and relative Boltzmann weights larger than 10^{-3}.

n	E_n^1	E_n^{high}	N_{config}
2	−11.655	−7.8393	6
4	−52.850	−41.380	953
10	−190.84	−179.36	796
20	−441.19	−429.72	216
100	−2 614.99	−2 611.09	4
500	−14 440.8	−14 431.6	2
1000	−30 031.6		1

gies of the equilibrium structures retained for the averaging of the calculated IR spectra are listed in Table II.

The basic idea of our IR-frequency calculations is to add the first and second order frequency shifts to the experimental monomer frequencies corresponding to each normal mode. A novel aspect in the present calculations, as compared to previous applications of our approach, is that the second order frequency shifts couple the considered normal mode not only with all other fundamental modes but also with their closest overtones, thus explicitly accounting also for Fermi resonances. However, it should be stressed that the first order frequency shifts remain unaffected. Concretely, the presence of the overtones implies that in Eq. (5) the fundamental frequencies ω_r appear as multiples, too. Intuitively, one might expect the additional resonant contributions to simply increase the frequency shifts, but this is not the case. In fact, they achieve a fine tuning of the total frequency shifts.

The beneficial effect of including the overtones can be judged by the example of the ν_1 mode in the case of the most stable isomer of the size $n=100$. The corresponding average first order frequency shift equals -17 cm^{-1}. Discarding $2\nu_2$, $3\nu_2$, and $2\nu_4$ (the overtones to be coupled with ν_1), the second order shift amounts to -150 cm^{-1}, while including these overtones results in -102 cm^{-1}. Having in view that the frequency shift from gas to crystalline solid is -126 cm^{-1}, by neglecting the couplings to the overtones the total frequency shift appears to be overestimated due to the second order contributions.

In the case of $2\nu_4$, where the gas to crystalline solid frequency shift is 73 cm^{-1}, the tremendous importance of including the overtones is even more apparent. The calculated average first order frequency shift for the most stable isomer of size $n=100$ is found to be 8 cm^{-1}. By not considering the overtone coupling, the second order shift results to be negative (-18 cm^{-1}), yielding a negative total shift, whereas, by including the effect of the overtones, the second order shift amounts to 32 cm^{-1}, resulting in a positive total frequency shift, as expected.

Another aspect worth mentioning is that the line spectrum for a given cluster size was averaged over the whole ensemble of computed cluster configurations. The cluster distribution according to the binding energies was assumed to be of Boltzmann type, corresponding to an equilibrium temperature of 200 K.

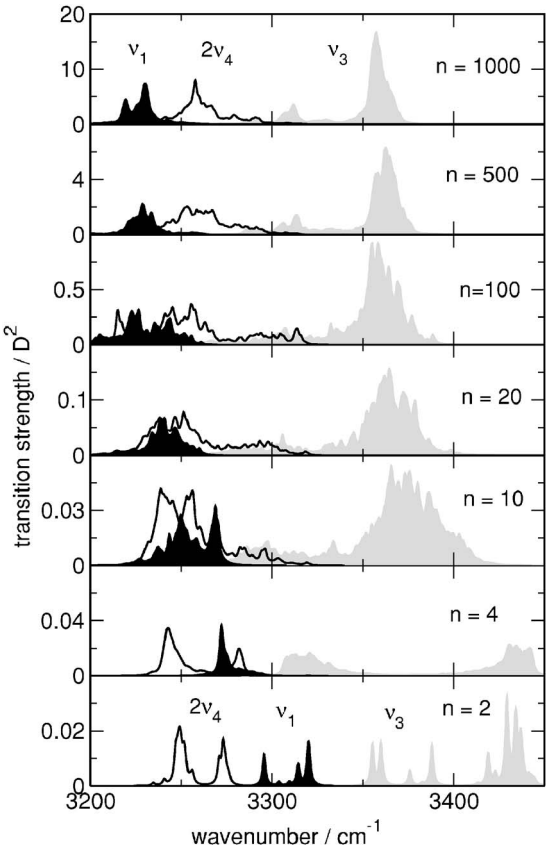

FIG. 6. Calculated IR spectra of ammonia clusters of the sizes indicated. The different modes $2\nu_4$, ν_1, and ν_3 are marked in white, black, and gray, respectively.

Figure 6 shows the ensemble-averaged IR spectra for the considered NH_3 clusters obtained by applying our perturbative frequency shift approach to the nondegenerate symmetric stretch mode ν_1, the doubly degenerate asymmetric stretch mode ν_3, and the overtone $2\nu_4$ of the doubly degenerate asymmetric bending mode. While the two NH-stretching modes exhibit the expected redshift caused by the hydrogen bonded system, the overtone of the asymmetric bending vibration shows a nearly constant behavior. It is also interesting to note that the redshift of the two NH-stretching modes is more pronounced for the small cluster sizes between $n=2$ and $n=10$ compared to that of the larger clusters. In conclusion, the results clearly demonstrate that there is a mixing between the redshifting ν_1 mode and nearly constant $2\nu_4$ mode which starts already around $n=10$ and is definitely over after $n=100$. We note that the intensities are not reliable because of the intramolecular force field of the monomer. To come close to the experimental values[28] one has to divide the given numbers by 100.

The main role in the crossing of ν_1 and $2\nu_4$ can be ascribed again to the second order frequency shifts. For the most stable isomers of sizes $n=10$, 20, and 100, the average first and second order contributions corresponding to ν_1 are $(-7,-12,-17)$ cm^{-1} and $(-76,-89,-102)$ cm^{-1}, respectively. It is apparent that both the largest contributions and the shift increase originate from the second order. As for $2\nu_4$, the average first and second order contributions for the same isomers are $(10,9,8)$ cm^{-1} and $(30,32,32)$ cm^{-1}, respec-

tively. Thus, the main explanation for the crossing of ν_1 and $2\nu_4$ modes results from the finding that, as opposed to ν_1, both the first and second order frequency shifts for $2\nu_4$ are very little sensitive to the cluster size, rendering a roughly constant total frequency shift.

V. DISCUSSION

The measured spectra of Fig. 3 alone did not allow us to derive some conclusions about the way in which the position of the three bands, involved in the investigated wave number region, changed. All measured cluster sizes exhibit a peak of large intensity at 3385 cm^{-1}, two peaks at 3220 and 3260 cm^{-1}, and some weaker intensities in the range of 3320 cm^{-1}. From the comparison of the result of the largest clusters with the condensed phase we know which modes these peaks correspond to. From the comparison of the smallest cluster with results of the single molecule only the position of the ν_3 could be obtained in an unambiguous way.

The calculations of Fig. 6, however, provide this answer. The problem here is how we can trust the results in view of the fact that we have to deal with the spectrum of a complicated hydrogen bonded manifold of up to 1000 molecules. Firstly there is the reliability of the interaction potential. We use for simplicity an effective two-body potential which has been fitted to liquid properties. It will not be very reliable for small clusters. Secondly, we have to find the correct minimum configuration and eventually account for the different isomers which will contribute. We do that in the present approach by averaging over a set of isomers. Thirdly, we have to calculate the frequency shift in a reliable way. We apply perturbation theory with degenerate states included. This has the advantage of being able to include also the coupling to the overtone, but it is per definition not so well suited for strong coupling cases. Fourthly, the intramolecular force field is not able to reproduce the measured monomer intensities. This will mainly affect the intensities but not the positions.

With all these caveats in mind, we will compare the measurements with the calculations for selected cluster sizes, the largest, the smallest, and one in the middle. The results are shown in Fig. 7. Although the agreement between experiment and theory is only qualitatively correct, it is good enough to assign the measured spectra and to pin down the origin of the measured peaks. It is obvious that the feature at 3385 cm^{-1} has to be attributed to the asymmetric stretch mode ν_3. The peak at the smallest size measured is a little bit broader and more structured than those of the other two sizes. These details are well reproduced by the calculations. For the two larger cluster sizes the absolute shift is predicted to be a bit too large by about 20 cm^{-1} and the width is too narrow compared to the experiment. But it is definitely clear that these peaks correspond to the ν_3 mode.

The more interesting region is that of the overlapping $2\nu_4$ and ν_1 bands. At the largest cluster size $\langle n\rangle = 989$ the peak at 3215 cm^{-1} is caused by the symmetric stretching ν_1 mode and the peak at 3260 cm^{-1} has to be attributed to the overtone of the asymmetric bending mode $2\nu_4$. This is also the assignment which follows from the results of the condensed phase. A very interesting result is that obtained for $\langle n\rangle = 80$. Here theory and experiment agree in the sense that in both cases a broad spectrum without specific structures is observed. The reason is a crossover of the redshifting symmetric stretch mode ν_1 and the nearly constant overtone of the asymmetric bending mode $2\nu_4$. They completely mix in this size range. At the smallest cluster size measured, $\langle n\rangle = 8$, the most redshifted peak at 3230 cm^{-1} originated from the overtone of the asymmetric bending mode $2\nu_4$. The peak at 3260 cm^{-1}, however, is, according to the calculation, already caused by a mixture of the $2\nu_4$ bending and the symmetric stretching mode ν_1. Surprisingly, the weaker peak at 3320 cm^{-1} is due to the ν_3 mode and not to the ν_1 mode whose monomer frequencies lie in this range. This result definitely clarifies that the peak structure of the experiment in the wave number range from 3200 to 3300 cm^{-1} which looks very similar has, however, to be traced back to different vibrational modes for different cluster sizes. According to the calculations, the mixing already starts around $n=8$ and is finished after $n=100$. We note that this interpretation of the origin of the lines for the large clusters is in agreement with the general interpretation of the corresponding spectra of the aerosol particles[12] and the condensed phase.[6,9] It is also in agreement with the results of the coherent anti-Stokes Raman spectroscopy (CARS) spectra of ammonia clusters in the size range of several tens of molecules which exhibit broad spectra and a peak of the ν_1 mode around 3204 cm^{-1}.[14]

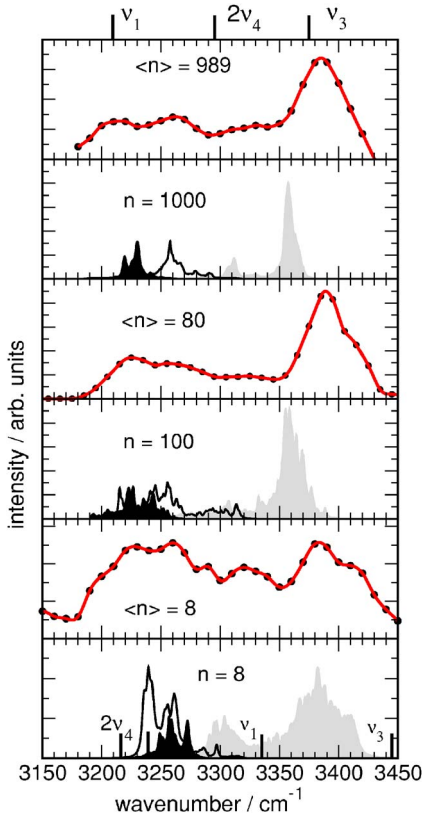

FIG. 7. (Color online) Comparison of measured and calculated spectra of ammonia clusters for the sizes indicated. In the calculations the different modes $2\nu_4$, ν_1, and ν_3 are marked in white, black, and gray, respectively. The bars at the bottom and the top indicate the positions of the vibrational modes of the monomer and the solid, respectively.

VI. CONCLUSIONS

In conclusion, we measured the evolution of IR spectra of ammonia clusters in the range of the NH-stretching vibrations as function of their size between $n=8$ and $n=1000$. By combining photofragment spectroscopy with the size determination by doping the ammonia cluster with sodium atoms, reliable results have been obtained. The experiments are accompanied by calculations of the vibrational spectra which are based on a model which allows us to include the coupling to the overtones of the different modes. From this calculation we definitely know the correct assignment of the spectra. In the size dependence of these spectra, there occurs a very interesting exchange in the wave number positions of the symmetric stretch vibration ν_1 with the overtone of the asymmetric bending motion $2\nu_4$ between $n=10$ and 100. Our calculations clearly demonstrate that the coupling between the ground state and the overtones is responsible for this crossing of the redshifting ν_1 and the nearly constant $2\nu_4$ mode. This is similar to the Fermi resonances which had already been evoked to explain part of the ammonia monomer spectra[4] and those of liquid ammonia.[9] Apparently, it is also operating in ammonia clusters in the complete size range covered by the present experiment and the accompanying calculations.

ACKNOWLEDGMENTS

This work was supported by the Deutsche Forschungsgemeinschaft in SFB 357 and GK 782 and by the Alexander-von-Humboldt-Stiftung in the "Forschungskooperation Europa." We are grateful to Martin A. Suhm, Yaqian Liu, and Ruth Signorell for useful discussion and copies of their data.

[1] M. L. Clapp and R. E. Miller, Icarus **105**, 529 (1993).
[2] I. Olovsson and D. H. Templeton, Acta Crystallogr. **12**, 832 (1959).
[3] W. S. Benedict, E. D. Plyler, and E. D. Tidwell, J. Chem. Phys. **32**, 32 (1960).
[4] R. Angstl, H. Finsterhözl, H. Frunder, D. Illig, D. Papoušek, P. Pranca, K. N. Rao, H. W. Schröter, and Š. Urban, J. Mol. Spectrosc. **114**, 454 (1985).
[5] O. S. Binbrek and A. Anderson, Chem. Phys. Lett. **15**, 421 (1972).
[6] A. Bromberg, S. Kimel, and A. Ron, Chem. Phys. Lett. **46**, 262 (1977).
[7] J. S. Holt, D. Sadoskas, and C. J. Pursell, J. Chem. Phys. **120**, 7153 (2004).
[8] T. Kume, S. Sasaki, and H. Shimizu, J. Raman Spectrosc. **32**, 383 (2001).
[9] M. Schwartz and C. H. Wang, J. Chem. Phys. **59**, 5258 (1973).
[10] F. Huisken and T. Pertsch, Chem. Phys. **126**, 213 (1988).
[11] Y. Liu, M. A. Suhm, and P. Botschwina, Phys. Chem. Chem. Phys. **6**, 4642 (2004).
[12] M. Jetzki, A. Bonnamy, and R. Signorell, J. Chem. Phys. **120**, 11775 (2004).
[13] M. N Slipchenko, K. E. Kuyanov, B. G. Sartakov, and A. F. Vilesov, J. Chem. Phys. **124**, 241101 (2006).
[14] H. D. Barth and F. Huisken, J. Chem. Phys. **87**, 2549 (1987).
[15] T. A. Beu and U. Buck, J. Chem. Phys. **114**, 7853 (2001).
[16] T. A. Beu and U. Buck, J. Chem. Phys. **114**, 7848 (2001).
[17] M. F. Vernon, D. J. Krajnovich, H. S. Kwok, J. M. Lisy, Y. R. Shen, and Y. T. Lee, J. Chem. Phys. **77**, 47 (1982).
[18] C. Steinbach, P. Andersson, J. K. Kazimirski, V. Buch, and T. A. Beu, J. Phys. Chem. A **108**, 6165 (2004).
[19] C. Bobbert, S. Schütte, C. Steinbach, and U. Buck, Eur. Phys. J. D **19**, 183 (2002).
[20] U. Buck, X. J. Gu, C. Lauenstein, and A. Rudolph, J. Chem. Phys. **92**, 6017 (1990).
[21] U. Buck and I. Ettischer, J. Chem. Phys. **108**, 33 (1998).
[22] O. F. Hagena, Surf. Sci. **106**, 101 (1981).
[23] O. F. Hagena, Z. Phys. D: At., Mol. Clusters **4**, 291 (1987).
[24] U. Buck and F. Huisken, Chem. Rev. (Washington, D.C.) **100**, 3863 (2000).
[25] U. Buck and C. Lauenstein, J. Chem. Phys. **92**, 4250 (1990).
[26] V. Buch, S. Bauerecker, J. P. Devlin, U. Buck, and J. K. Kazimirski, Int. Rev. Phys. Chem. **23**, 375 (2004).
[27] T. A. Beu, C. Steinbach, and U. Buck, Eur. Phys. J. D **27**, 223 (2003).
[28] I. Kleiner, L. R. Brown, G. Tarrago, Q.-L. Kou, N. Picqué, G. Guelachvili, V. Dana, and J.-Y. Mandin, J. Mol. Spectrosc. **193**, 46 (1999).
[29] T. A. Beu, Z. Phys. D: At., Mol. Clusters **31**, 95 (1994).
[30] T. A. Beu and K. Takeuchi, J. Chem. Phys. **103**, 6394 (1995).
[31] R. W. Impey and M. L. Klein, Chem. Phys. Lett. **104**, 579 (1984).
[32] M. Diraison, G. J. Martyna, and M. E. Tuckerman, J. Chem. Phys. **111**, 1096 (1999).
[33] U. Buck and B. Schmidt, J. Chem. Phys. **98**, 9410 (1993).
[34] E. B. Wilson, J. C. Decius, and P. C. Cross, *Molecular Vibrations* (McGraw-Hill, New York, 1955).
[35] A. R. Hoy, I. M. Mills, and G. Strey, Mol. Phys. **24**, 1265 (1972).
[36] Y. Morino, K. Kuchitsu, and S. Yamamoto, Spectrochim. Acta, Part A **24**, 335 (1968).
[37] J. W. Reed and P. M. Harris, J. Chem. Phys. **35**, 1730 (1961).